



## Review Article

# State-of-the-art Prostate Imaging

Hakan Ayyildiz, Artur Salmaslioglu, Atadan Tunaci, Sukru Mehmet Erturk

Department of Radiology, Istanbul University, Istanbul Faculty of Medicine, Istanbul, Türkiye

### ABSTRACT

Prostate cancer is one of the most common cancers in men. In addition to methods such as prostate-specific antigen test, digital rectal examination, and transrectal ultrasonography, magnetic resonance imaging has an important role for accurate and reproducible diagnosis. However, guidance in targeted biopsies and recent use in determining localization for treatment increase its importance. Due to technical difficulties, patient tolerance, and differences in interpretation, the prostate imaging reporting and data system recommends preparations for the patient and magnetic resonance imaging techniques. However, techniques continue to be developed to improve the diagnosis rate and image quality. In our article, patient preparation before imaging and techniques were tried to be discussed in detail. In addition, current approaches in biparametric magnetic resonance imaging and radiomics and new techniques such as T1 and T2 mapping will be mentioned.

**Keywords:** Magnetic resonance imaging, multiparametric magnetic resonance imaging, prostate cancer

Please cite this article as "Ayyildiz H, Salmaslioglu A, Tunaci A, Erturk SM. State-of-the-art Prostate Imaging. Med Bull Sisli Etfal Hosp 2023;57(2):153–162".

Prostate cancer is the second most common cancer in men and accounts for 15% of all cancers.<sup>[1]</sup> In Western countries, prostate cancer is the most common cancer in men.<sup>[1]</sup> The most important risk factor for prostate cancer is age. Most patients are individuals over the age of 65. Prostate-specific antigen (PSA) test, although not specific, allows early diagnosis of prostate cancer. In this way, an increasing proportion of patients can be diagnosed at an early stage.<sup>[2]</sup> Nevertheless, PSA can be elevated in many benign conditions (e.g., benign prostatic hyperplasia). However, in recent studies, it has been shown that PSA screening studies do not contribute to survival and even lead to overdiagnosis and overtreatment.<sup>[3]</sup> Digital rectal examination, on the other hand, can detect tumors over 0.2 mL, and its sensitivity is very low.

Recently, prostate cancer is accepted as a multifocal disease, in which a dominant focus and other focus coexist when detected. From a clinical point of view, clinically in-

significant (Gleason  $\leq 6$ ) or clinically significant (Gleason  $\geq 7$ ) cancers should be distinguished.

Multiparametric prostate magnetic resonance imaging (MpMRI) has been developing and becoming more important in the diagnosis and treatment of prostate cancer in recent years. In the past, it was performed with abdominal imaging for staging purposes and to detect extraprostatic extension. The use of morphological and functional sequences provided a more effective diagnosis. MpMRI has begun to play a role in the degree of aggressiveness of prostate cancer, thus in the diagnosis of clinically significant and clinically insignificant prostate cancer. Recent data suggest that targeted biopsies combined with MpMRI detect more clinically significant cancers and less clinically insignificant cancers than standard biopsies.<sup>[4]</sup> However, because of the high false-negative rate of targeted biopsies, it is still stated that they should be performed together with standard biopsies.<sup>[5]</sup>

**Address for correspondence:** Hakan Ayyildiz, MD. Department of Radiology, Istanbul University, Istanbul Faculty of Medicine, Istanbul, Türkiye

**Phone:** +90 534 973 43 49 **E-mail:** hakanayyildiz77@gmail.com

**Submitted Date:** December 22, 2022 **Revised Date:** January 02, 2023 **Accepted Date:** January 19, 2023 **Available Online Date:** June 20, 2023

©Copyright 2023 by The Medical Bulletin of Sisli Etfal Hospital - Available online at [www.sislietfaltip.org](http://www.sislietfaltip.org)

**OPEN ACCESS** This is an open access article under the CC BY-NC license (<http://creativecommons.org/licenses/by-nc/4.0/>).



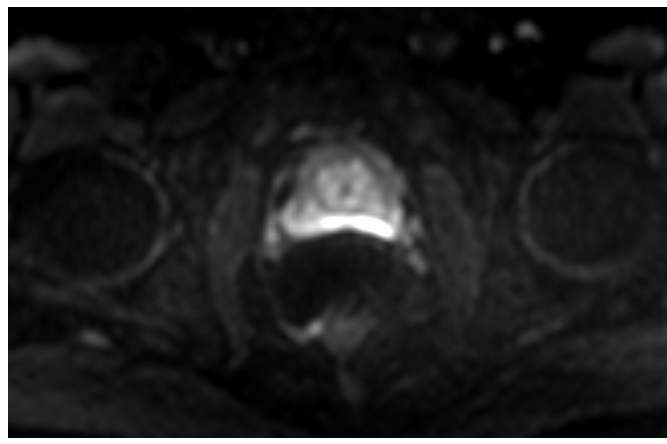


**Figure 1.** In the diffusion magnetic resonance imaging image obtained with the B1400, diffusion restrictions in the posterior peripheral zone of the prostate caused by gas in the rectum are observed.

### The Prostate Imaging Reporting and Data System (PI-RADS)

PI-RADS version 1 was published in 2012 by the European Society of Urogenital Radiology to standardize prostate MR reports due to rapid advances in prostate MR.<sup>[6]</sup> PI-RADS v1 contained limitations with improvements in MpMRI, and PI-RADS version 2.0 was published in 2016.<sup>[7]</sup> In 2019, the PI-RADS committee published PI-RADS v2.1 because PI-RADS v2.0 contains some inconsistencies in the studies carried out since its publication and it needs to be developed.<sup>[8]</sup>

### Patient Preparation

In PI-RADS v2.1, emptying the rectum before extraction is the only recommendation in patient preparation (Fig. 1). Apart from this, the use of enemas and antispasmodic agents is optional.

After the use of hyoscine butylbromide, an antispasmodic agent, improvement was observed in T2-weighted (T2W) images in studies published by Ullrich et al.<sup>[9]</sup> and Slough et al.<sup>[10]</sup> but no improvement was observed in the study published by Roethke et al.<sup>[11]</sup> There was no improvement in diffusion-weighted imaging (DWI).<sup>[9-11]</sup>

Coskun et al.<sup>[12]</sup> reported in their study that the use of enemas did not reduce artifacts in DWI. However, Plodeck et al.<sup>[13]</sup> showed that the use of enemas resulted in an improvement in DWI artifacts. Coskun et al.<sup>[12]</sup> worked at a b value of 1500 s/mm<sup>2</sup> in the DWI, and Plodeck et al.<sup>[13]</sup> worked at 1000 s/mm<sup>2</sup>. 3 Tesla MR was used in both studies, and the number of patients was similar in both studies (Coskun et al.: 117 patients, Plodeck et al.: 114 patients). Lim et al.<sup>[14]</sup> found no significant difference in artifacts in T2W images of enema use in their study.

### Optimal Time

A period of 6–8 weeks is recommended for magnetic resonance imaging after biopsy.<sup>[15,16]</sup> However, in some publications, it is stated that even after 6 weeks, the absorption of hemorrhage is insufficient.<sup>[17,18]</sup> (Fig. 2). Choi et al.<sup>[19]</sup> showed

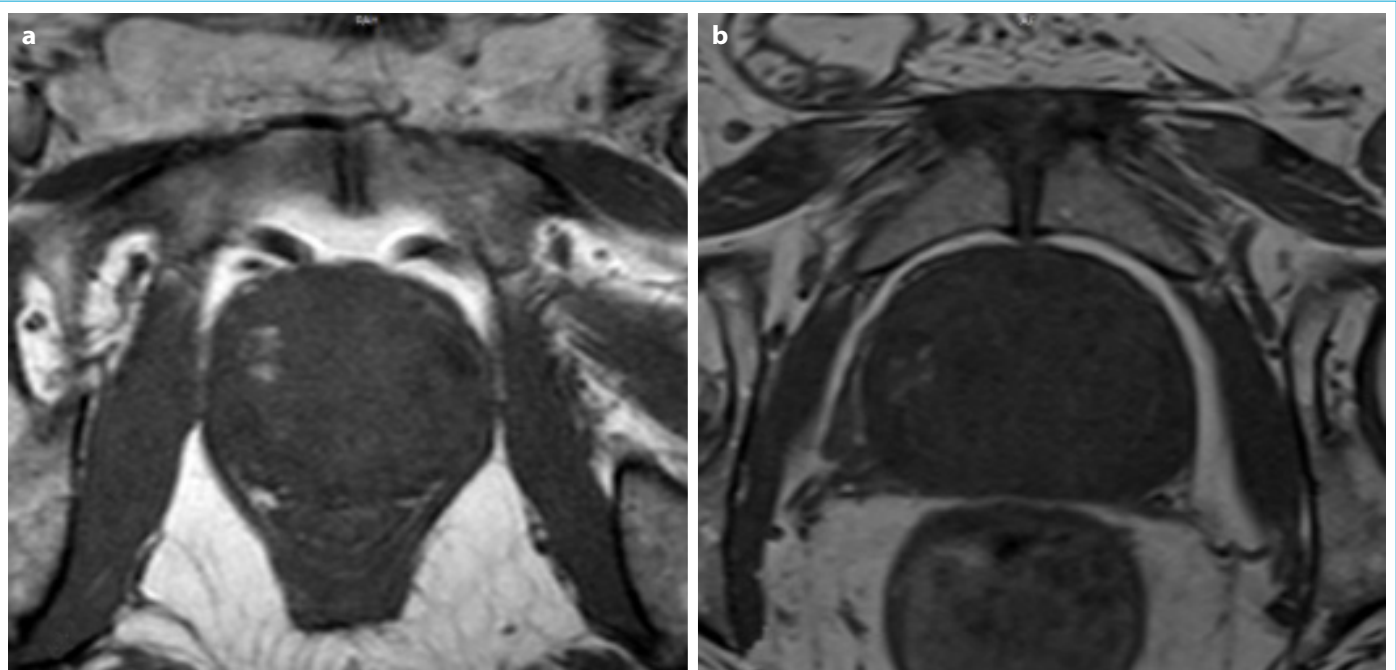


**Figure 2.** Post-biopsy magnetic resonance imaging (MRI) (a) and 6 months later MRI (b) of the same patient are shown. In these two T1W images, the MR obtained 6 months after the biopsy (b) shows that although the bleeding area is partially resolved, slight signal intensity changes persist in the lateral and posterior regions.

that staging in magnetic resonance imaging was not associated with the post-biopsy interval. It is also thought that the amount of bleeding is not related to the interval.<sup>[17,19]</sup> There is no consensus on this matter.

Ejaculation causes the collapse of seminal vesicles, also, it can cause difficulties in their evaluation.<sup>[20]</sup> Furthermore, the T2 signal in the peripheral zone decreases after ejaculation.<sup>[21]</sup> Some centers recommend 3 days of sexual abstinence, but there is no recommendation in PI-RADS v2.1 due to insufficient evidence.

### Technical Specifications

According to PI-RADS v2.1, prostate MRI should be performed at a minimum of 1.5 Tesla.<sup>[22]</sup> Signal-to-noise ratio (SNR) is higher at 3 Tesla (T) MRI. Furthermore, 3T MRI proves better temporal and spatial resolution. However, 1.5 T continues to be a preferable option in examinations that may have susceptibility artifacts (e.g., hip prosthesis).

### Endorectal Coil (ERC)

The purpose of the use of an ERC is to increase SNR. The use of ERC is usually required on older, 1.5 Tesla MRIs.<sup>[22]</sup> In addition, it has been shown in recent studies that ERC increases SNR in DWI, especially in the peripheral zone, and better reflects anatomical details in T2-weighted imaging in 3T MRIs. In patients using ERC, the diagnosis rate of smaller and less aggressive lesions increased and the rate of missed lesions decreased.<sup>[23]</sup> Dhatt et al.<sup>[24]</sup> showed that the use of ERC in Gleason 4+3 and higher lesions did not cause a significant difference in the diagnosis rate, but the diagnosis rate was higher in the case of ERC use in Gleason 3+4 lesions. Tirumani et al.<sup>[25]</sup> did not find any significant difference in the diagnosis rates of ERC use in the extraprostatic spread and seminal vesicle invasion in their study.

There is no standard recommendation in PI-RADS v2.1 about the use of ERC. The use of ERC varies from center to center depending on the features of the center's MR device, usability, time, and patient preference.

### Treatment in Prostate Cancer with Magnetic Resonance Imaging

Recently, the opportunity to treat with magnetic resonance imaging has emerged with the wide-ranging magnetic resonance imaging technology.<sup>[26]</sup> In our institute, wide-bore MRI studies are supported with scholarship support (Fig. 3).

### T2-Weighted Imaging

T2W imaging (T2W) is the major pulse sequence in prostate MR examination. It should be done with Rapid Im-

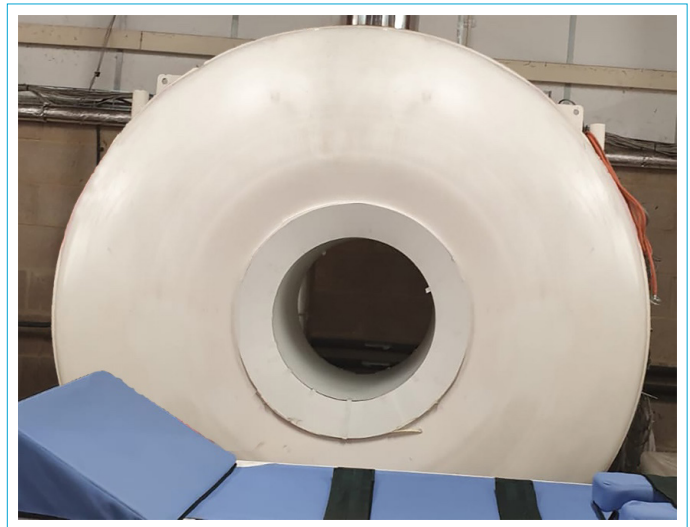


**Figure 3.** Wide-bore magnetic resonance imaging technology at our institute.

aging with Refocused Echoes technique, turbo spin echo (TSE), and fast spin echo are other types of this technique. In these techniques, the long echo train causes blur artifacts (Fig. 4).

According to PI-RADS v2.1, at least two sections should be examined, one of which is in the axial plane. The axial plane can be taken according to the straight axial or long axis of the prostate gland (Fig. 5). The examination of the long axis of the prostate gland is considered to be better, but the straight axial plane is more applicable for technologists.<sup>[27,28]</sup>

The isotropic 3D sequence can be made in addition to the 2D images. The major advantages of 3D imaging are the lower partial volume effect and higher resolution. The 3D examination is thought to be useful in identifying the extraprostatic extension and the capsule of BPH nodules. However, it is more sensitive to motion artifacts. However, when acquiring 3D images, TR time can be shortened to reduce shooting time; however, this may influence T1 weight (Fig. 6).

### Diffusion-Weighted Imaging (DWI)

DWI has gained even more importance with the popularization of biparametric MR. Spin echo planar imaging (EPI) technique is recommended in PI-RADS v2.1. The plan should be similar to T2-weighted imaging. This technique has a high SNR ratio and is less susceptible to motion artifacts due to its rapidity. However, it is more sensitive to susceptibility artifacts. Another technique, single-shot TSE, is less sensitive to susceptibility artifacts in DWI imaging, although signal loss and artifacts are its major handicaps.

“Reduced field-of-view”-DWI is a recent new technique

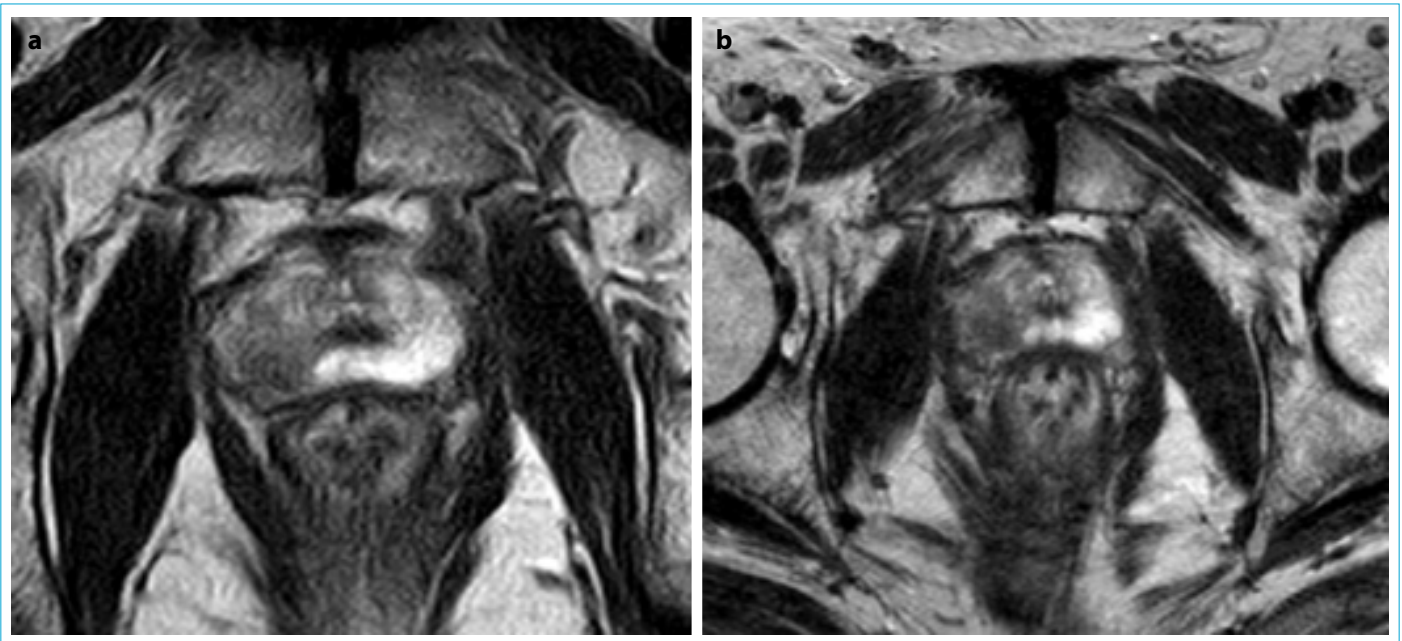


**Figure 4.** Blur artifact caused by the long echo train is visible on T2 Imaging (a). Better image was obtained when the imaging was adjusted with the appropriate parameters (b).

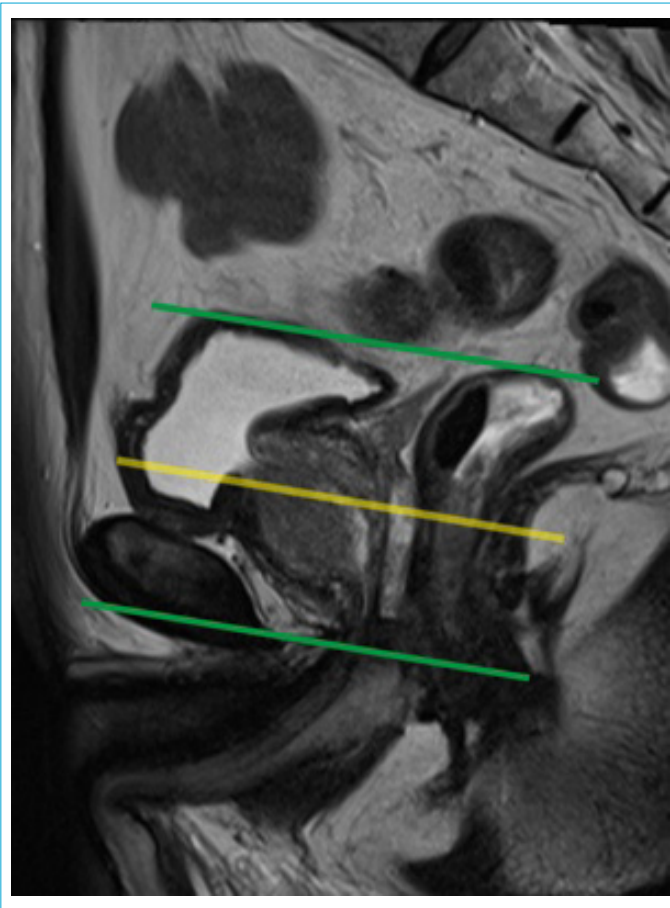


**Figure 5.** In the sagittal T2 image, the orientation of the axial image is seen based on the prostate long axis. It should be scanned starting from the superior seminal vesicle. The green lines represent the scan ranges. The yellow line is the reference line.

(Fig. 7). In recent studies, it has been shown that the technique provides an increase in image quality in anatomical distortion and susceptibility artifact compared to standard single-shot EPI (ssEPI).<sup>[28]</sup> Two recent articles have reported that there is no significant difference from the standard DWI technique in detecting prostate cancer.<sup>[29,30]</sup>

Another disadvantage of the ssEPI DWI is the blurring artifact, which becomes more apparent as the magnetic field strength increases.<sup>[31]</sup> It is thought that this effect is mostly due to  $T_2^*$  attenuation. Although blurring artifacts can be reduced with a parallel imaging technique, it remains one of the major problems of the ssEPI DWI sequence. Multi-shot EPI sequence shortens the shot length as it fills the k-space with multiple excitations, thus reducing blurring artifacts but being relatively sensitive to motion artifacts due to phase difference.<sup>[32]</sup>

In prostate MRI,  $1500\text{--}2000\text{ s/mm}^2$  is generally used as a high b value in daily practice. Insufficient suppression is observed at low b values, and a decrease in anatomical resolution is observed at high b values (such as  $3000\text{--}5000\text{ s/mm}^2$ ). Rosenkratz et al.<sup>[33]</sup> reported  $1500\text{--}2500\text{ s/mm}^2$  as the optimal value for the detection of prostate cancer in their study on computer-assisted b values. Similarly, Vural et al.<sup>[34]</sup> reported that in the detection of prostate cancer in computer-assisted b values,  $2000\text{ s/mm}^2$  and  $3000\text{ s/mm}^2$  were similar and superior to  $1500\text{ s/mm}^2$  in both. However, Zhang et al.<sup>[35]</sup> reported that the  $3000\text{ s/mm}^2$  images they obtained natively, provided higher AUCs than  $1000\text{ s/mm}^2$  and  $2000\text{ s/mm}^2$  in the detection of prostate cancer. Pro-

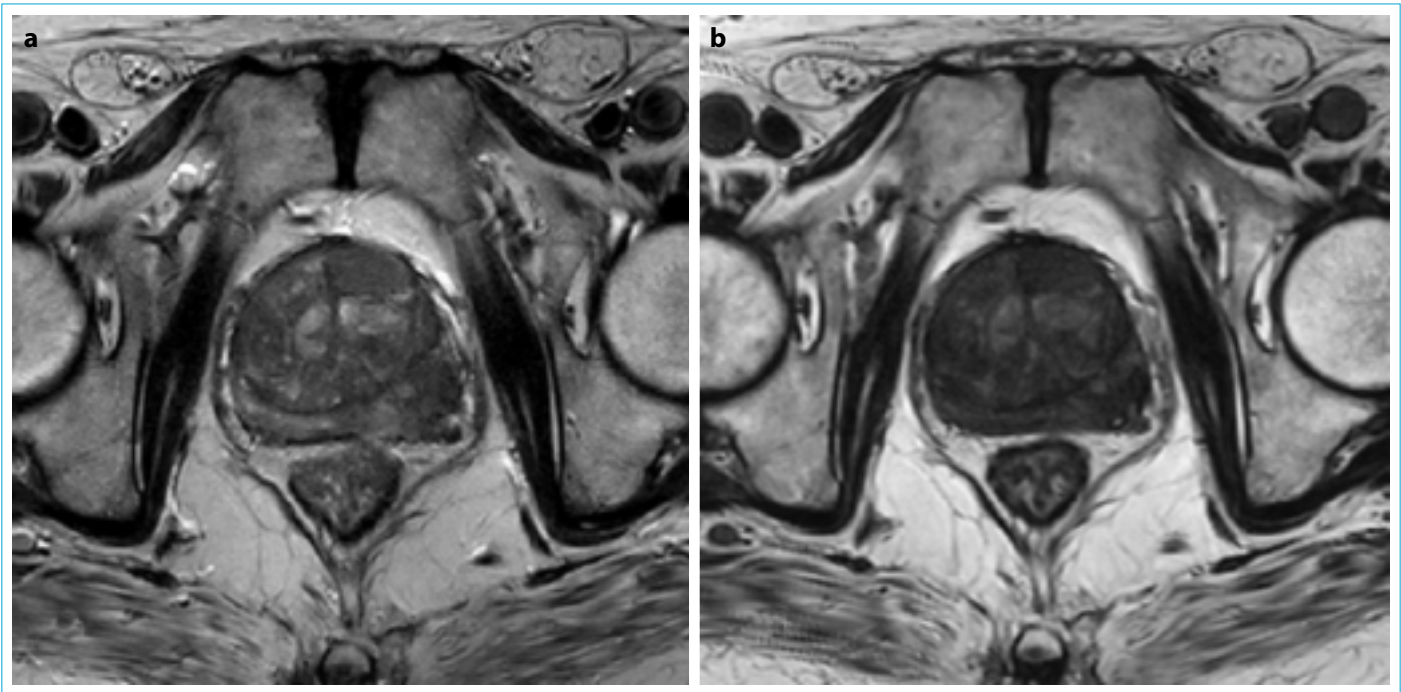


**Figure 6.** 2D T2-weighted image (a) and 3D isotropic T2-weighted image (b) of the lesion with extraprostatic extension in the left peripheral zone. While T2 images are obtained in 3D images, an increase in T1 weight can be observed. (The case was obtained from Medmar Imaging Center with permission).

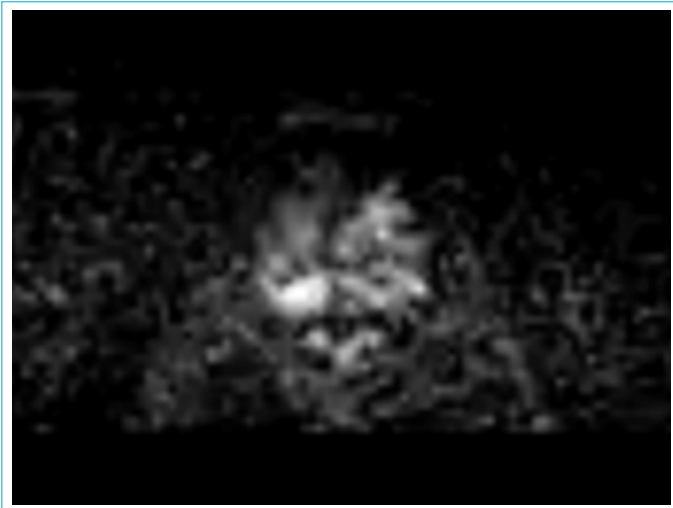


**Figure 7.** Peripheral zone tumor is seen in the reduced field of view image. (The case was obtained from Medmar Imaging Center with permission).

spective and multicenter studies are needed to prove the diagnostic performance of high B values.

PI-RADS v2.1 recommendation is to have a minimum b value of  $\geq 1400$  s/m<sup>2</sup> for DWI. However,  $\leq 1000$  s/m<sup>2</sup> is recommended for apparent diffusion coefficient (ADC) calculation. The reason for this is the diffusion kurtosis effect that may occur at high b values (Fig. 8). Recently, it has been investigated whether ADC histogram analyses pro-

vide a higher diagnostic rate than standard ADC. Tamada et al.<sup>[36]</sup> showed that 0–10. Percentiles achieved the best results in serial MR scans. Zhang et al.<sup>[37]</sup> demonstrated that the bi-exponential model (IVIM) provides better performance than the mono-exponential model. However, it is thought that it does not provide better performance than other studies.<sup>[38,39]</sup> There was no significant difference between the stretched exponential model and the mono-exponential model.<sup>[40]</sup> Diffusion kurtosis imaging is another model studied, and it has been found to have better diagnostic performance than the mono-exponential model in some studies, worse in some, and similar diagnostic performance in others.<sup>[40,41]</sup> In current studies, it is seen that these models are not clearly good compared to the mono-exponential model and need to be improved.

### Dynamic Contrast Enhancement (DCE)

DCE-MRI is acquired by taking serial images T1W images with 2D or 3D gradient echo techniques after bolus injection of gadolinium-based contrast agents with low-molecular-weight chelation. Fat suppression techniques and subtraction images are recommended. Due to current technological developments, 3D imaging is applied more often, which increases image quality.

In prostate cancer, an increase in angiogenesis and capillary permeability is observed. As a result, early-focal enhancement and washout are seen.<sup>[42]</sup> Detailed parameters were

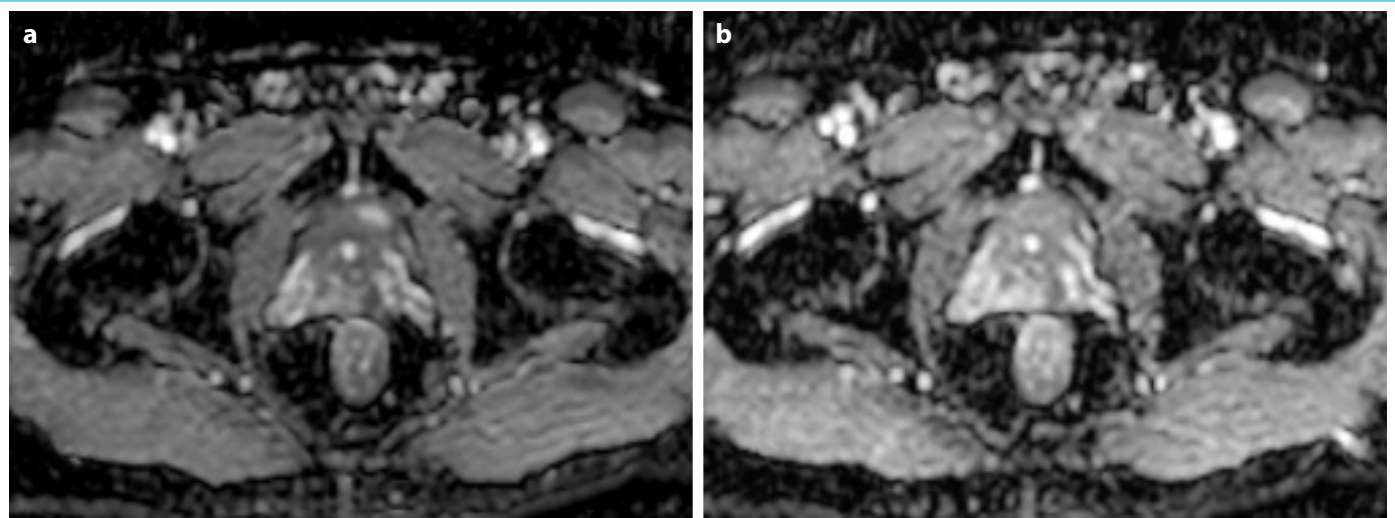


**Figure 8.** Images of apparent diffusion coefficient (ADC)-b800 (a) and ADC-b1400 (b) are shown. Peripheral zone tumor is more demonstrative in B800 ADC because of the diffusion kurtosis effect that occurs at high b values.

available in PI-RADS v2 because of the importance of DCE-MRI standardization. The imaging plan used for DWI should be used for DCE-MRI. Slice thickness should be 3 mm, with no gaps. The field of view should cover the prostate gland and seminal vesicle. Minimum temporal resolution should be  $\leq 15$  s for each image. For gadolinium-based contrast agents (GBCAs), a dose of 0.1 mmol/kg and an injection rate of 2–3 cc/s are recommended. Total examination time should be at least 2 min with no gaps in between. DCE imaging can be a “safety-net” examination in DWI when adequate SNR is not obtained or contains artifacts. In PI-RADS v2.1, no changes were made in the technical recommendations, some recommendations were made for biparametric MRI (bpMRI) performed without DCE due to some limitations of DCE.

As the magnetic field strength increases (3 Tesla), SNR increase. There are also improvements in spatial and temporal resolution. Shooting time is shortened. Furthermore, the relaxation time of GBCA decreases. For these reasons, the contrast difference between prostate cancer and the surrounding tissue increases and the contribution of DCE-MRI to the diagnosis increases.<sup>[43]</sup> Image quality is improved using ERC, especially in the peripheral zone around the rectum wall, but ERC is not preferred in most centers for patient comfort and additional costs.<sup>[44]</sup>

DCE-MRI can be evaluated with qualitative, semi-quantitative, and quantitative methods. The qualitative method is the visual assessment of the evaluated operator. Four different types have been defined in PIRADS v1 as progressive (Type 1), plateau (Type 2), washout (Type 3), and non-diagnostic (Type 0). The semi-quantitative technique is based on mathematical computation in the signal-time

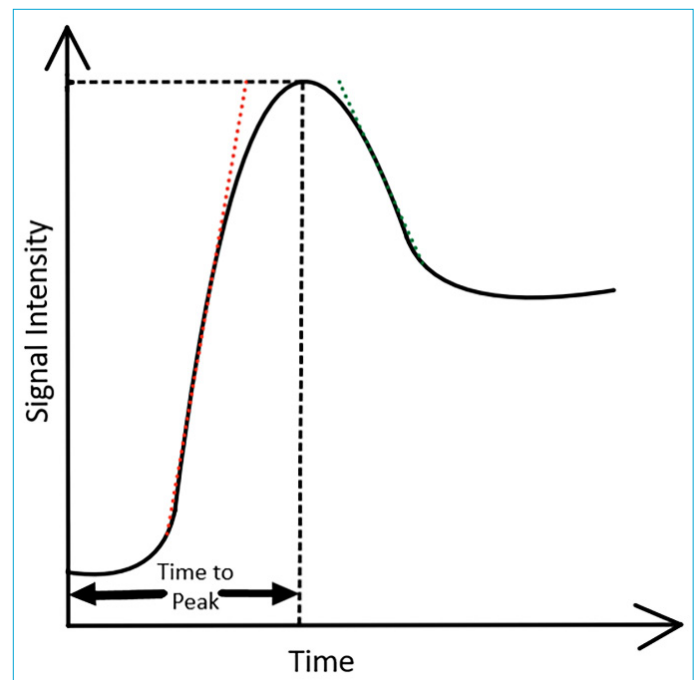


**Figure 9.** Graphic overview of semi-quantitative dynamic contrast enhancement-magnetic resonance imaging parameters. The red-dotted line represents the wash-in rate, and the green-dotted line represents the wash-out rate.

curve (Fig. 9). Mathematical models used to smooth the contrasting signals yield diagnostically useful kinetic parameters. This approach can be functional for heterogeneous enhancements, but frequently used compartment models may not be compatible with accurate spatial and temporal spread.<sup>[45]</sup> Quantitative analysis allows measures such as permeability and blood flow. This is one of its main advantages. The challenge of quantitative analysis is the

accurate measurement of arterial input function (AIF). The gold standard in selecting a specific AIF is serial blood collection after contrast agent injection. However, since this method is invasive, the average AIF values of the population are generally used. Cardiac output differences can create differences in AIF. AIF may vary from person to person and even between shots in the same person.<sup>[46]</sup>

## bpMRI

DCE may have a limited role in prostate imaging. bpMRI provides lower cost and faster acquisition.<sup>[47]</sup> In addition, because the contrast is not used, negative side effects are avoided. For this reason, bpMRI, an MRI of the prostate without DCE, is being studied with increasing interest. In some meta-analyses, bpMRI has achieved comparable diagnostic rates compared to mpMRI.<sup>[48]</sup> Nevertheless, the number of readers may be limited in these meta-analyses. In addition, these meta-analyses did not study low-quality images, to which DCE contributed relatively. According to PI-RADS v2.1, there are three indications for DCE:

- Identification of PI-RADS 3 lesions that contain clinically significant prostate cancer
- Assist in T2 and DWI imaging with suboptimal image quality
- Assisting radiologists with less experience.
- In addition, PIRADS v2.1 suggests opting for mpMRI in certain situations:
  - Patients with negative previous biopsies and suspected elevated PSA
  - Rapid PSA doubling time or change in clinical status in active surveillance
  - Patients with previous bpMRI imaging and clinical suspicion
  - Patients receiving prostate interventions or drug-hormone therapy, who may have altered prostate anatomy
  - Biopsy-naïve men with a family history, genetic predisposition, or a higher than average risk
  - Conditions that may reduce DWI or T2 image quality, such as a hip implant.

There is still no standardized reporting system for bpMRI, which leads to heterogeneity in meta-analyses.<sup>[49]</sup> More multicenter meta-analyses are needed for the development of bpMRI.

## T1 and T2 Mapping

T1 and T2 mapping is based on the calculation of T1 and T2 relaxation times of tissues and the creation of color maps. It is obtained by collecting data at several TE times

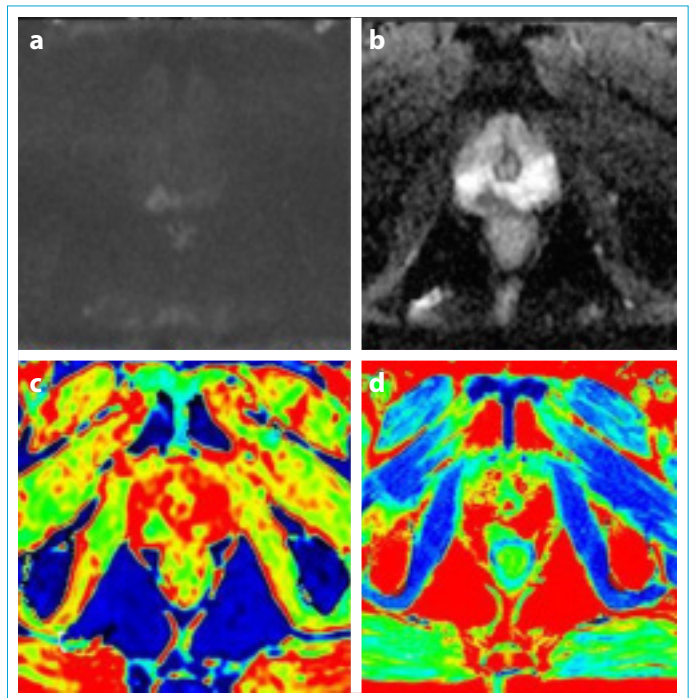


**Figure 10.** Diffusion-weighted imaging (a) and apparent diffusion coefficient (b) imaging shows a tumor localized in the right peripheral zone mid-gland, posteromedial. T1 mapping (c) and T2 mapping (d) images are shown as well. The diagnosis of this patient after the biopsy was adenocarcinoma.

in a TR interval. The average relaxation time of voxels at different TE times is calculated mathematically. The modified Look-Locker inversion recovery (MOLLI) technique, which is an inversion recovery technique, can be used for T1 mapping, and the EPI technique, which is a spin echo technique, can be used for T2 mapping (Fig. 10).

T1 and T2 relaxation times may vary with many parameters such as gender, age, exercise, and hemoglobin. Significant differences were observed in T1 and T2 times in some of the malignancies, and it is thought that this difference can be used especially in prostate and breast cancers.<sup>[50]</sup>

## Radiomics

Radiomics is a relatively new field of medicine that is created by extracting quantitative features from images that are invisible to the naked eye and, supporting clinical decisions. Features such as size, shape, and first-order texture are obtained from computed tomography, magnetic resonance imaging, or other modalities. Numerous studies have been published in tumoral and non-tumoral diseases related to radiomics in the last decade. Some of these studies are on prognosis prediction, while others are on diagnostic and genomic prediction. Despite recent advances in MpMRI, 25% of tumors in the transition zone still cannot be diagnosed. In studies published in recent years, it has

been shown that radiomics determines prostate cancer diagnosis and location with high sensitivity and specificity.<sup>[51]</sup> In addition, in recent years, many studies have been published on the role of radiomics in determining PIRADS, Gleason score, the presence of extraprostatic extension, response to tumor therapy, and prognosis predictions.<sup>[51]</sup> There is an increasing interest in radiomics, and multi-center studies are needed for its development.

## Conclusion

Prostate imaging techniques, including T2 imaging, DWI, DCE, radiomics, and T1 and T2 mapping techniques, have revolutionized the field of prostate imaging. These advanced imaging modalities offer improved accuracy, sensitivity, and specificity in detecting and characterizing prostate diseases. In addition, advancements in artificial intelligence and machine learning hold great promise in further enhancing image interpretation and quantitative analysis. Incorporating these cutting-edge techniques into clinical practice can lead to better diagnosis, risk stratification, treatment planning, and patient management. As the field of prostate imaging continues to evolve, radiologists play a pivotal role in staying updated with the latest advancements to provide the best care for their patients.

## Disclosures

**Acknowledgments:** This study was funded by Scientific Research Projects Coordination Unit of our university. Project number: 36427.

**Peer-review:** Externally peer-reviewed.

**Conflict of Interest:** None declared.

**Authorship Contributions:** Concept – H.A., A.S., A.T., S.M.E.; Design – H.A., A.S., A.T., S.M.E.; Supervision – H.A., A.S., A.T., S.M.E.; Fundings – H.A., A.S., A.T., S.M.E.; Materials – H.A., S.M.E.; Data collection &/or processing – H.A., S.M.E.; Analysis and/ or interpretation – H.A., S.M.E.; Literature search – H.A., S.M.E.; Writing – H.A.; Critical review – A.T., S.M.E.

## REFERENCES

1. Ferlay J, Soerjomataram I, Dikshit R, Eser S, Mathers C, Rebelo M, et al. Cancer incidence and mortality worldwide: sources, methods and major patterns in GLOBOCAN 2012. *Int J Cancer* 2015;136:E359–86. [\[CrossRef\]](#)
2. Catalona WJ, Richie JP, Ahmann FR, Hudson MA, Scardino PT, Flanigan RC, et al. Comparison of digital rectal examination and serum prostate specific antigen in the early detection of prostate cancer: results of a multicenter clinical trial of 6,630 men. *J Urol* 1994;151:1283–90. [\[CrossRef\]](#)
3. Dahm P, Neuberger M, Ilic D. Screening for prostate cancer: shaping the debate on benefits and harms. *Cochrane Database Syst Rev* 2013:Ed000067. [\[CrossRef\]](#)
4. Ahmed HU, El-Shater Bosaily A, Brown LC, Gabe R, Kaplan R, Parmar MK, et al. Diagnostic accuracy of multi-parametric MRI and TRUS biopsy in prostate cancer (PROMIS): a paired validating confirmatory study. *Lancet* 2017;389:815–22. [\[CrossRef\]](#)
5. Tan N, Margolis DJ, Lu DY, King KG, Huang J, Reiter RE, et al. Characteristics of detected and missed prostate cancer foci on 3-T multiparametric MRI using an endorectal coil correlated with whole-mount thin-section histopathology. *AJR Am J Roentgenol* 2015;205:W87–92. [\[CrossRef\]](#)
6. Barentsz JO, Richenberg J, Clements R, Choyke P, Verma S, Villeirs G, et al; European Society of Urogenital Radiology. ESUR prostate MR guidelines 2012. *Eur Radiol* 2012;22:746–57. [\[CrossRef\]](#)
7. Weinreb JC, Barentsz JO, Choyke PL, Cornud F, Haider MA, Macura KJ, et al. PI-RADS prostate imaging - reporting and data system: 2015, version 2. *Eur Urol* 2016;69:16–40. [\[CrossRef\]](#)
8. Turkbey B, Rosenkrantz AB, Haider MA, Padhani AR, Villeirs G, Macura KJ, et al. Prostate imaging reporting and data system version 2.1: 2019 update of prostate imaging reporting and data system version 2. *Eur Urol* 2019;76:340–51. [\[CrossRef\]](#)
9. Ullrich T, Quentin M, Schmaltz AK, Arsov C, Rubbert C, Blondin D, et al. Hyoscine butylbromide significantly decreases motion artefacts and allows better delineation of anatomic structures in mp-MRI of the prostate. *Eur Radiol* 2018;28:17–23. [\[CrossRef\]](#)
10. Slough RA, Caglic I, Hansen NL, Patterson AJ, Barrett T. Effect of hyoscine butylbromide on prostate multiparametric MRI anatomical and functional image quality. *Clin Radiol* 2018;73:e9–216. [\[CrossRef\]](#)
11. Roethke MC, Kuru TH, Radbruch A, Hadaschik B, Schlemmer HP. Prostate magnetic resonance imaging at 3 Tesla: is administration of hyoscine-N-butyl-bromide mandatory? *World J Radiol* 2013;5:259–63. [\[CrossRef\]](#)
12. Coskun M, Mehralivand S, Shih JH, Merino MJ, Wood BJ, Pinto PA, et al. Impact of bowel preparation with Fleet's™ enema on prostate MRI quality. *Abdom Radiol (NY)*. 2020;45:4252–9. [\[CrossRef\]](#)
13. Plodeck V, Radosa CG, Hübner HM, Baldus C, Borkowetz A, Thomas C, et al. Rectal gas-induced susceptibility artefacts on prostate diffusion-weighted MRI with epi read-out at 3.0 T: does a preparatory micro-enema improve image quality? *Abdom Radiol* 2020;45:4244–51. [\[CrossRef\]](#)
14. Lim C, Quon J, McInnes M, Shabana WM, El-Khodary M, Schieda N. Does a cleansing enema improve image quality of 3T surface coil multiparametric prostate MRI? *J Magn Reson Imaging* 2015;42:689–97. [\[CrossRef\]](#)
15. White S, Hricak H, Forstner R, Kurhanewicz J, Vigneron DB, Zaloudek CJ, et al. Prostate cancer: effect of postbiopsy hemorrhage on interpretation of MR images. *Radiology* 1995;195:385–90. [\[CrossRef\]](#)
16. Ko YH, Song PH, Moon KH, Jung HC, Cheon J, Sung DJ. The optimal timing of post-prostate biopsy magnetic resonance imaging to guide nerve-sparing surgery. *Asian J Androl* 2014;16:280–4. [\[CrossRef\]](#)



17. Tamada T, Sone T, Jo Y, Yamamoto A, Yamashita T, Egashira N, et al. Prostate cancer: relationships between postbiopsy hemorrhage and tumor detectability at MR diagnosis. *Radiology* 2008;248:531–39. [\[CrossRef\]](#)
18. Sharif-Afshar AR, Feng T, Koopman S, Nguyen C, Li Q, Shkoliar E, et al. Impact of post prostate biopsy hemorrhage on multiparametric magnetic resonance imaging. *Can J Urol* 2015;22:7698–702.
19. Choi MH, Jung SE, Park YH, Lee JY, Choi Y-J. Multiparametric MRI of prostate cancer after biopsy: little impact of hemorrhage on tumor staging. *Investig Magn Reson Imaging* 2017;21:139–47. [\[CrossRef\]](#)
20. Kabakus IM, Borofsky S, Mertan FV, Greer M, Daar D, Wood BJ, et al. Does abstinence from ejaculation before prostate MRI improve evaluation of the seminal vesicles? *AJR Am J Roentgenol* 2016;207:1205–09. [\[CrossRef\]](#)
21. Medved M, Sammet S, Yousuf A, Oto A. MR imaging of the prostate and adjacent anatomic structures before, during, and after ejaculation: qualitative and quantitative evaluation. *Radiology* 2014;271:452–60. [\[CrossRef\]](#)
22. Puryško AS, Baroni RH, Giganti F, Costa D, Renard-Penna R, Kim CK, et al. PI-RADS version 2.1: a critical review, from the AJR special series on radiology reporting and data systems. *AJR Am J Roentgenol* 2021;216:20–32. [\[CrossRef\]](#)
23. Lee G, Oto A, Giurcanu M. Prostate MRI: is endorectal coil necessary?—A review. *Life (Basel)* 2022;12:569. [\[CrossRef\]](#)
24. Dhatt R, Choy S, Co SJ, Ischia J, Kozłowski P, Harris AC, et al. MRI of the prostate with and without endorectal coil at 3 T: correlation with whole-mount histopathologic Gleason score. *AJR Am J Roentgenol* 2020;215:133–41. [\[CrossRef\]](#)
25. Tirumani SH, Suh CH, Kim KW, Shinagare AB, Ramaiya NH, Fennessy FM. Head-to-head comparison of prostate MRI using an endorectal coil versus a non-endorectal coil: meta-analysis of diagnostic performance in staging T3 prostate cancer. *Clin Radiol* 2020;75:157. [\[CrossRef\]](#)
26. de Marini P, Cazzato RL, Garnon J, Shaygi B, Koch G, Auloge P, et al. Percutaneous MR-guided prostate cancer cryoablation technical updates and literature review. *BJR Open* 2019;1:20180043. [\[CrossRef\]](#)
27. Caglic I, Barrett T. Optimising prostate mpMRI: prepare for success. *Clin Radiol* 2019;74:831–40. [\[CrossRef\]](#)
28. Thierfelder KM, Scherr MK, Notohamiprodjo M, Weiß J, Dietrich O, Mueller-Lisse UG, et al. Diffusion-weighted MRI of the prostate: advantages of Zoomed EPI with parallel-transmit-accelerated 2D-selective excitation imaging. *Eur Radiol* 2014;24:3233–41. [\[CrossRef\]](#)
29. Brendle C, Martirosian P, Schwenzer NF, Kaufmann S, Kruck S, Kramer U, et al. Diffusion-weighted imaging in the assessment of prostate cancer: comparison of zoomed imaging and conventional technique. *Eur J Radiol* 2016;85:893–900. [\[CrossRef\]](#)
30. Tamada T, Ream JM, Doshi AM, Taneja SS, Rosenkrantz AB. Reduced field-of-view diffusion-weighted magnetic resonance imaging of the prostate at 3 Tesla: comparison with standard echo-planar imaging technique for image quality and tumor assessment. *J Comput Assist Tomogr* 2017;41:949–56. [\[CrossRef\]](#)
31. Scheenen TW, Rosenkrantz AB, Haider MA, Fütterer JJ. Multiparametric magnetic resonance imaging in prostate cancer management: current status and future perspectives. *Invest Radiol* 2015;50:594–600. [\[CrossRef\]](#)
32. Dai E, Zhang Z, Ma X, Dong Z, Li X, Xiong Y, et al. The effects of navigator distortion and noise level on interleaved EPI DWI reconstruction: a comparison between image- and k-space-based method. *Magn Reson Med* 2018;80:2024–32. [\[CrossRef\]](#)
33. Rosenkrantz AB, Parikh N, Kierans AS, Kong MX, Babb JS, Taneja SS, et al. Prostate cancer detection using computed very high b-value diffusion-weighted imaging: how high should we go? *Acad Radiol* 2016;23:704–11. [\[CrossRef\]](#)
34. Vural M, Ertaş G, Onay A, Acar Ö, Esen T, Sağlıcan Y, et al. Conspicuity of peripheral zone prostate cancer on computed diffusion-weighted imaging: comparison of cDWI1500, cDWI2000, and cDWI3000. *Biomed Res Int* 2014;2014:768291. [\[CrossRef\]](#)
35. Zhang K, Shen Y, Zhang X, Ma L, Wang H, An N, et al. Predicting prostate biopsy outcomes: a preliminary investigation on screening with ultrahigh b-value diffusion-weighted imaging as an innovative diagnostic biomarker. *PLoS One* 2016;11:e0151176. [\[CrossRef\]](#)
36. Tamada T, Dani H, Taneja SS, Rosenkrantz AB. The role of whole-lesion apparent diffusion coefficient analysis for predicting outcomes of prostate cancer patients on active surveillance. *Abdom Radiol (NY)* 2017;42:2340–45. [\[CrossRef\]](#)
37. Zhang YD, Wang Q, Wu CJ, Wang XN, Zhang J, Liu H, et al. The histogram analysis of diffusion-weighted intravoxel incoherent motion (IVIM) imaging for differentiating the Gleason grade of prostate cancer. *Eur Radiol* 2015;25:994–1004. [\[CrossRef\]](#)
38. Bao J, Wang X, Hu C, Hou J, Dong F, Guo L. Differentiation of prostate cancer lesions in the Transition Zone by diffusion-weighted MRI. *Eur J Radiol Open* 2017;4:123–28. [\[CrossRef\]](#)
39. Barbieri S, Brönnimann M, Boxler S, Vermathen P, Thoeny HC. Differentiation of prostate cancer lesions with high and with low Gleason score by diffusion-weighted MRI. *Eur Radiol* 2017;27:1547–55. [\[CrossRef\]](#)
40. Toivonen J, Merisaari H, Pesola M, Taimen P, Boström PJ, Pahikkala T, et al. Mathematical models for diffusion-weighted imaging of prostate cancer using b values up to 2000 s/mm<sup>2</sup>: correlation with Gleason score and repeatability of region of interest analysis. *Magn Reson Med* 2015;74:1116–24. [\[CrossRef\]](#)
41. Suo S, Chen X, Wu L, Zhang X, Yao Q, Fan Y, et al. Non-Gaussian water diffusion kurtosis imaging of prostate cancer. *Magn Reson Imaging* 2014;32:421–7. [\[CrossRef\]](#)
42. de Rooij M, Hamoen EH, Fütterer JJ, Barentsz JO, Rovers MM. Accuracy of multiparametric MRI for prostate cancer detection: a meta-analysis. *AJR Am J Roentgenol* 2014;202:343–51. [\[CrossRef\]](#)

43. Hagberg GE, Scheffler K. Effect of  $r_1$  and  $r_2$  relaxivity of gadolinium-based contrast agents on the  $T_1$ -weighted MR signal at increasing magnetic field strengths. *Contrast Media Mol Imaging* 2013;8:456–65. [\[CrossRef\]](#)
44. Turkbey B, Merino MJ, Gallardo EC, Shah V, Aras O, Bernardo M, et al. Comparison of endorectal coil and nonendorectal coil T2W and diffusion-weighted MRI at 3 Tesla for localizing prostate cancer: correlation with whole-mount histopathology. *J Magn Reson Imaging* 2014;39:1443–8. [\[CrossRef\]](#)
45. Port RE, Knopp MV, Hoffmann U, Milker-Zabel S, Brix G. Multicompartment analysis of gadolinium chelate kinetics: blood-tissue exchange in mammary tumors as monitored by dynamic MR imaging. *J Magn Reson Imaging* 1999;10:233–41. [\[CrossRef\]](#)
46. Lavini C, Verhoeff JJ. Reproducibility of the gadolinium concentration measurements and of the fitting parameters of the vascular input function in the superior sagittal sinus in a patient population. *Magn Reson Imaging* 2010;28:1420–30. [\[CrossRef\]](#)
47. Alver KH, Yagci AB, Utebey AR, Turk NS, Ufuk F. Comparison of multiparametric and fast mri protocols in detecting clinically significant prostate cancer and a detailed cost analysis. *J Magn Reson Imaging* 2022;56:1437–47. [\[CrossRef\]](#)
48. Greenberg JW, Koller CR, Casado C, Triche BL, Krane LS. A narrative review of biparametric MRI (bpMRI) implementation on screening, detection, and the overall accuracy for prostate cancer. *Ther Adv Urol* 2022;14:17562872221096377. [\[CrossRef\]](#)
49. Belue MJ, Yilmaz EC, Daryanani A, Turkbey B. Current status of biparametric MRI in prostate cancer diagnosis: literature analysis. *Life* 2022;12:804. [\[CrossRef\]](#)
50. Hepp T, Kalmbach L, Kolb M, Martirosian P, Hilbert T, Thaiss WM, et al. T2 mapping for the characterization of prostate lesions. *World J Urol* 2022;40:1455–61. [\[CrossRef\]](#)
51. Cutaia G, La Tona G, Comelli A, Vernuccio F, Agnello F, Gagliardo C, et al. Radiomics and prostate MRI: current role and future applications. *J Imaging* 2021;7:34. [\[CrossRef\]](#)